Physical Property Changes as a Monitor of Pelagic Carbonate Diagenesis: an Empirically Derived Diagenetic Model for Atlantic Ocean Basins[1]

Jens Grützner[2] and Jürgen Mienert[3]

ABSTRACT

A new physical model of carbonate diagenesis has been derived based on physical property measurements from 81 DSDP/ODP (Deep-Sea Drilling Project/Ocean Drilling Project) drill sites in the Atlantic Ocean. Changing depth gradients of porosity, bulk density, P-wave velocity (vertical and horizontal), and acoustic impedance characterize five successive diagenetic stages: (1) compaction of ooze, (2) breakage and dissolution of fossil tests, (3) formation of chalk through precipitation of calcite, (4) cementation, and (5) compaction of calcite crystals. Age-depth information from the drill sites was used to calculate the average duration of these processes in Atlantic Ocean basins. The model can predict carbonate sediment physical properties down to a burial depth of 1000 m. The model is presented for both lab and in-situ conditions and thus can serve as a standard for comparison with lab, log, and seismic measurements. An acoustic impedance vs. age curve derived from the model allows estimation of the initial and present-day diagenetic potential of carbonate sediments and chalk reservoirs.

INTRODUCTION

Half of the area of the sea floor (180 million km^2) is covered with pelagic calcareous oozes (e.g., Berger, 1974). The diagenetic conversion of these unconsolidated oozes starts after a stage of simple mechanical compaction by overburden pressure at shallow depth; cementation is the dominant process in deeper burial diagenesis. Cementation, in turn, is controlled by pressure solution of foraminiferal tests and coccolith elements and by reprecipitation of secondary calcite on larger crystals (Schlanger and Douglas, 1974). Solution and reprecipitation may occur simultaneously and are controlled by factors such as time, temperature, pressure, pore water chemistry, and host rock lithology (e.g., Matter et al., 1975). Rates of solution and reprecipitation are highly site and taxa selective. To cover all stages of diagenesis, Schlanger and Douglas (1974, p. 133) introduced the concept of the diagenetic potential that they qualitatively defined as "the length of the diagenetic pathway left for the original dispersed foraminiferal-nannoplankton assemblage to traverse before it reaches the very low free energy level of a crystalline mosaic."

Several studies have described changes of physical and acoustic properties of carbonate sediments during diagenesis (e.g., Schlanger and Douglas, 1974; Scholle, 1977; Kim et al., 1985; Urmos and Wilkens, 1993; Brasher and Vagle, 1996). In general, the loss in porosity in carbonates during lithification is accompanied by an increase in P-wave velocity and bulk density. A first diagenetic model for physical property changes in pelagic carbonate sediments that takes into account observations on mineralogical transformations was deduced from an ooze-chalk-limestone sequence drilled at the Magellan Rise in the central North Pacific (Schlanger and Douglas, 1974). Schlanger and Douglas (1974) calculated average values of porosity, density, and velocity for ooze, chalk, and limestone zones. Since then, further investigations of physical property data from ooze-chalk-limestone sequences have been performed in areas with pure and continuous carbonate sedimentation in the Pacific Ocean, such as the Ontong Java Plateau (van der Lingen and Packham, 1975; Milholland et al., 1980; Kim et al., 1985) or the Manihiki Plateau (Boyce, 1976a). The different models derived from

[1]Manuscript received February 5, 1998; revised manuscript received February 2, 1999; final acceptance March 16, 1999.

[2]GEOMAR Forschungszentrum für marine Geowissenschaften, Wischhofstr. 1-3, D-24148 Kiel, Germany; e-mail: jgruetzner@geomar.de

[3]GEOMAR Forschungszentrum für marine Geowissenschaften, Wischhofstr. 1-3, D-24148 Kiel, Germany. Now at Department of Geology, University of Tromsø, Dramsveien 201,N-9037 Tromsø, Norway.

We acknowledge the financial support of the "Deutsche Forschungsgemeinschaft (DFG)." The manuscript was improved by the comments of J. W. Schmoker, R. E. Garrison, and one anonymous reviewer.

these studies deviate from one another because they are restricted by the specific sedimentary conditions in the examined regions; furthermore, most of these studies are limited by the fact that they refer to the descriptive DSDP/ODP (Deep-Sea Drilling Project/Ocean Drilling Project) categories ooze, chalk, and limestone rather than to diagenetic processes, such as compaction, solution, and reprecipitation. Because of the somewhat subjective nature of the DSDP/ODP classification (e.g., oozes are soft sediments easily deformed under the finger or broad spatula blade) it is often difficult to compare diagenetic processes at different localities (Urmos, 1994).

Modeling of the porosity loss in sediments with increasing burial depth has been of special interest to researchers because of its implications for hydrocarbon exploration. Predictive equations for the porosity decrease with depth in chalks have been derived for various regions of commercial interest in onshore and nearshore areas (e.g., Scholle, 1977; D'Heur, 1984; Sørensen et al., 1986; Mazullo and Harris, 1992; Brasher and Vagle, 1996). Much less work exists on deep-sea pelagic carbonate sediments, especially in the Atlantic Ocean. Based on DSDP data, Hamilton (1976) derived equations of porosity and density vs. depth for various types of deep-sea sediments, including carbonates; however, Hamilton's regression equations are based only on eight data points with 50 m separation. Additional detailed studies of physical property changes in carbonate sediments have become possible using the enhanced core recovery and higher resolution sampling obtained by the ODP (e.g., Bassinot et al., 1993; Urmos and Wilkens, 1993).

In this paper, we present an empirical physical model of carbonate diagenesis for the Atlantic Ocean. Our model is based on all available discrete velocity, bulk density, and porosity data measured on ooze, chalk, and limestone samples from 81 DSDP/ODP drill sites. The observed physical property changes were correlated to the mineralogical changes observed during carbonate diagenesis. The available stratigraphic information from drill sites has been used to estimate the average time of duration for different diagenetic stages. The model provides a standard that can be used to compare records from individual sites, enabling one to estimate the remaining diagenetic potential of sediments.

METHODS

The primary data set used in this study integrates physical property measurements performed on carbonate samples ($CaCO_3$ content >50%) from 81 DSDP/ODP drill sites in the Atlantic Ocean (Figure 1). The physical property records of each drill hole have been compared to the lithologic descriptions to select velocity, density, and porosity (vs. depth) values measured on ooze, chalk, and limestone samples. Additionally, the age of each sample was calculated from the stratigraphic information available for each site.

Bulk densities and porosities belong to the so-called index properties and were determined from measurements of sediment weights and volumes (wet and dry). Bulk density is defined as the weight of the wet saturated sediment divided by its volume. Porosity is defined as the volume of the pore space divided by the volume of the wet saturated sample and is expressed as a percentage. These measurements, as well as the necessary salt corrections, are described in detail by Boyce (1976b) and in the explanatory notes chapters of the DSDP/ODP initial reports.

Compressional wave (P-wave) velocity measurements are based on accurate measurements of the time for an acoustic signal to travel between a pair of sensors with known separation. Most of the velocity measurements used here have been obtained with the Hamilton Frame Velocimeter® (Boyce, 1973) during DSDP/ODP cruises. In soft sediment, the instrument was used to measure velocities on split cores through the core liner (perpendicular to the core axis). Hard samples were cut out of the core so that velocity measurements parallel and perpendicular to the core axis were possible. Beginning with ODP Leg 130 the Digital Sound Velocimeter® (Mayer et al., 1987) was used in addition to the Hamilton Frame Velocimeter. This instrument uses two pairs of transducers inserted into soft sediment to measure velocity in the *x*-(perpendicular to the core axis) and *z*-directions (along core).

To derive empirical models of physical property changes in Atlantic carbonate sediments, the selected data sets were treated in the following way.

Crossplots of density vs. porosity for each site were used to identify possible erroneous measurements. Outliers from the expected linear relationship between density and porosity were excluded from the data base.

Because the model should reflect "normal" sedimentary conditions in the Atlantic, measurements from areas with very slow and very rapid carbonate sedimentation also were excluded. These samples were identified by calculating the average sedimentation rate for each sample based on the available age/depth information. Only measurements from samples with sedimentation rates between 1 and 8 cm/k.y. since the time of deposition were considered for further calculations.

Velocity anisotropy (A_p) in percent was calculated from measurements of vertical (V_v) and horizontal

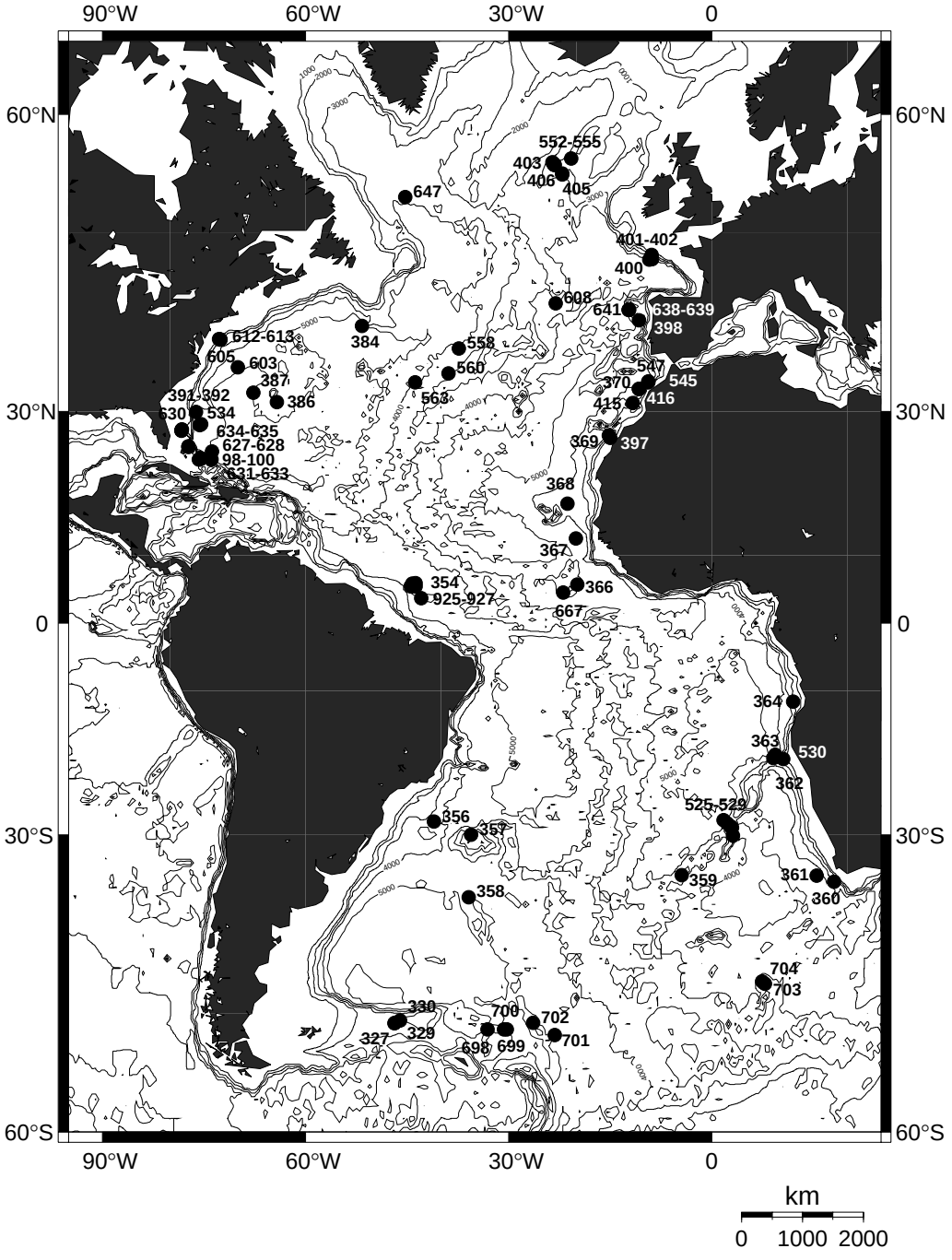

Figure 1—Locations of DSDP/ODP drill sites from which physical property data have been used in this study. Contours indicate water depth in 1000 m intervals.

(V_h) velocity on the same sample using the following definition of Carlson and Christensen (1977):

$$A_p = 200 \times \frac{\left(V_h - V_v\right)}{\left(V_h + V_v\right)}$$

Average values (with standard deviation) of measured (bulk density, porosity, velocity) and derived (age, impedance, anisotropy) physical properties were calculated for successive 40 m depth intervals (e.g., 0–40 m, 40–80 m, etc.). A total of 8880 measurements was used for the calculations. The number of data points for each parameter in each interval is given in Table 1. Below 1000 m, the number of available measurements drops to fewer than ten per depth interval; therefore, the derived model is restricted to the interval 0–1000 m below sea floor (mbsf).

To allow comparison of the derived model using measurements under laboratory conditions at 25°C and with those obtained under in-situ conditions (e.g., downhole logs, seismic velocities), the original model, which was based on laboratory data, has been adjusted to downhole temperature and pressure conditions. Laboratory measurements of sediment properties can differ from in-situ values because of (1) temperature changes, (2) pressure reduction, (3) decrease of sediment rigidity, and (4) mechanical porosity rebound (Hamilton, 1965, 1976). Porosity rebound resulting from reduction of overburden pressure after core recovery has commonly been assumed to have the most significant impact on laboratory measurements of physical properties (e.g., Hamilton, 1976). Crossplots have been widely used to derive in-situ values of density and velocity from the estimated porosity rebound (e.g., Shipley, 1983; Hempel et al., 1989); however, more recent studies (Marsters and Manghnani, 1993; Urmos and Wilkens, 1993; Urmos et al., 1993) have demonstrated that mechanical rebound in marine carbonate sediments is much smaller than the 5% maximum porosity increase predicted from the empirical rebound function of Hamilton (1976). Urmos et al. (1993) found that only minor corrections to adjust for hydraulic rebound of the pore fluids were needed to yield excellent agreement between log and laboratory porosities and densities. They also derived empirical laboratory velocity corrections by using differences in lab-to-log velocities at drill sites from ODP Leg 130. These new corrections were successfully tested for oozes and chalks recovered at ODP Sites 704, 722, and 762 (Urmos and Wilkens, 1993). In our study, the corrections described by Urmos et al. (1993) and Urmos and Wilkens (1993) were applied to adjust physical property measurements to in-situ conditions. The effects of hydraulic rebound on density and porosity were corrected by calculating the difference between laboratory and in-situ sea water densities for each site. Two corrections were applied to laboratory velocity data. The first correction was for in-situ temperature and pressure of the pore fluids using (Wyllie et al., 1956)

$$1/V_{corr} = 1/V_{meas} + \left[\left(\eta/V^{w}_{in\,situ}\right) - \left(\eta/V^{w}_{lab}\right)\right]$$

where η = fractional porosity, V_{corr} = temperature and pressure corrected velocity, V_{meas} = measured velocity, $V^{w}_{in\,situ}$ = velocity of sea water at in-situ temperature and pressure (using Mackenzie, 1981), and V^{w}_{lab} = velocity of sea water at laboratory temperature and pressure (using Mackenzie, 1981). The second correction applied was to correct the differences in elastic moduli and sediment rigidity by using (Urmos and Wilkens, 1993)

$$V_{in\,situ} = V_{corr} + 0.66 \times \left(1 - e^{-0.00208 \times d}\right)$$

where V_{corr} = temperature corrected velocity, $V_{in\,situ}$ = velocity under in-situ conditions, d = depth (in mbsf).

RESULTS AND DISCUSSION

Changes of Physical Properties with Depth

Figure 2 shows the variations of density, velocity, and porosity in carbonate sediments with burial depth after statistical evaluation of all recorded measurements. The negative linear correlation between porosity and bulk density leads to the mirror image seen in Figures 2a, b. Porosity decreases from 70% at the sea floor to values of less than 20% below 900 m burial depth, whereas bulk density increases in the same interval from 1.55 to 2.30 g/cm^3. The decrease in porosity also is accompanied by an increase in compressional wave velocity. Vertical velocity (perpendicular to the bedding plane) is approximately 1.5 km/s at the sea floor, generally increasing to 3.05 km/s below 900 m. The general trend in horizontal velocity (parallel to the bedding plane) is similar to that of vertical velocity; however, an increasing difference in absolute value with burial depth indicates increasing acoustic anisotropy. The graphs in Figure 2 demonstrate that there is no simple linear, exponential, or log function that can fit the data sets over the depth range of 0–1000 m. This is also illustrated in Figure 3, which compares porosity trends from three Atlantic sites for the upper 300 m burial depth with an exponential function derived by Hamilton (1976). The porosity approximation by Hamilton's curve fits the data quite well close to the sea floor and at greater depth, but in between there are zones of nearly constant porosity that differ from site to site.

The general trend in physical property changes with depth associated with increasing lithification is characterized by changing gradients with depth (Figure 2). This is more clearly seen in Figure 4, where the downhole trends for all parameters have been approximated by nine-term polynomial regression (coefficients provided in Table 2). For comparison, the relative portions of ooze, chalk, and limestone (from core descriptions) in different depth intervals are plotted in the background of the graph. For example, at 200 m depth about 80%

Table 1. Number of Measurements per Depth Interval Used for Statistical Evaluation

Depth Interval (m)	Number of Measurements				
	Density	Porosity	Horizontal Velocity	Vertical Velocity	Acoustic Anisotropy
0–40	168	158	129	119	101
40–80	161	155	135	111	97
80–120	192	181	146	105	95
120–160	181	169	146	97	92
160–200	185	173	161	54	51
200–240	187	183	126	34	30
240–280	134	124	96	27	15
280–320	122	120	114	42	37
320–360	148	138	127	88	81
360–400	112	102	85	62	62
400–440	112	108	74	57	51
440–480	139	136	84	64	64
480–520	135	135	87	74	72
520–560	137	132	91	80	75
560–600	106	104	60	59	52
600–640	93	86	43	30	30
640–680	67	66	21	15	13
680–720	74	76	32	22	22
720–760	91	87	62	41	41
760–800	90	92	87	66	66
800–840	67	66	64	57	57
840–880	49	48	43	36	36
880–920	21	22	25	22	22
920–960	12	12	13	11	11
Total No. Measurements	2783	2673	2051	1373	1273

of the examined samples were carbonate oozes, whereas the remaining 20% were described as chalks. The background composition data indicate that the transitions ooze/chalk and chalk/limestone on average occur at about 250 m and 700 m depth, respectively.

The ooze-to-chalk and chalk-to-limestone transitions are characterized by large gradient changes (Table 3, Figure 4). Although the ooze-to-chalk transition is characterized by changes to higher gradients, the top of the limestone interval marks a change to lower gradients. Additionally, marked changes in the slope of the velocity, density, and porosity curves (from high to low gradients) are visible within the ooze interval at about 70–100 m depth. Another change (from low to very high gradients) occurs at about 850–900 m depth, which is well within the limestone interval.

Although the changes caused by hydraulic rebound are very small (0.1–0.4%) for porosity and density measurements (not visible in Figures 2a, b) significant differences between laboratory and in-situ conditions are apparent in acoustic velocities (Figures 4c, d). The differences gradually increase from the sea floor to the chalk/limestone transition at 700 mbsf and decrease again in limestones; however, the general trends with burial depth do not change from lab to in-situ conditions.

A Physical Model of Carbonate Diagenesis

To correlate the observed physical property changes with diagenetic processes, we compared the physical property records with published data concerning the state of fossil preservation and textural changes with depth (e.g., Fischer et al., 1967; Wise, 1973; Schlanger and Douglas, 1974; Matter et al., 1975; Garrison, 1981; Audet, 1995; Borre et al., 1996). Numerous scanning electron micrographs from these studies have illustrated these changes. In this paper, we present scanning electron micrographs of carbonate samples from two localities at different depth intervals (Figure 5) to illustrate textural changes.

Based on the mineralogic information, it is possible to correlate each segment of the physical property graphs with a diagenetic process. For detailed comparison, we computed an acoustic impedance vs. depth curve (Figure 6). Acoustic impedance is the product of the average vertical velocity and

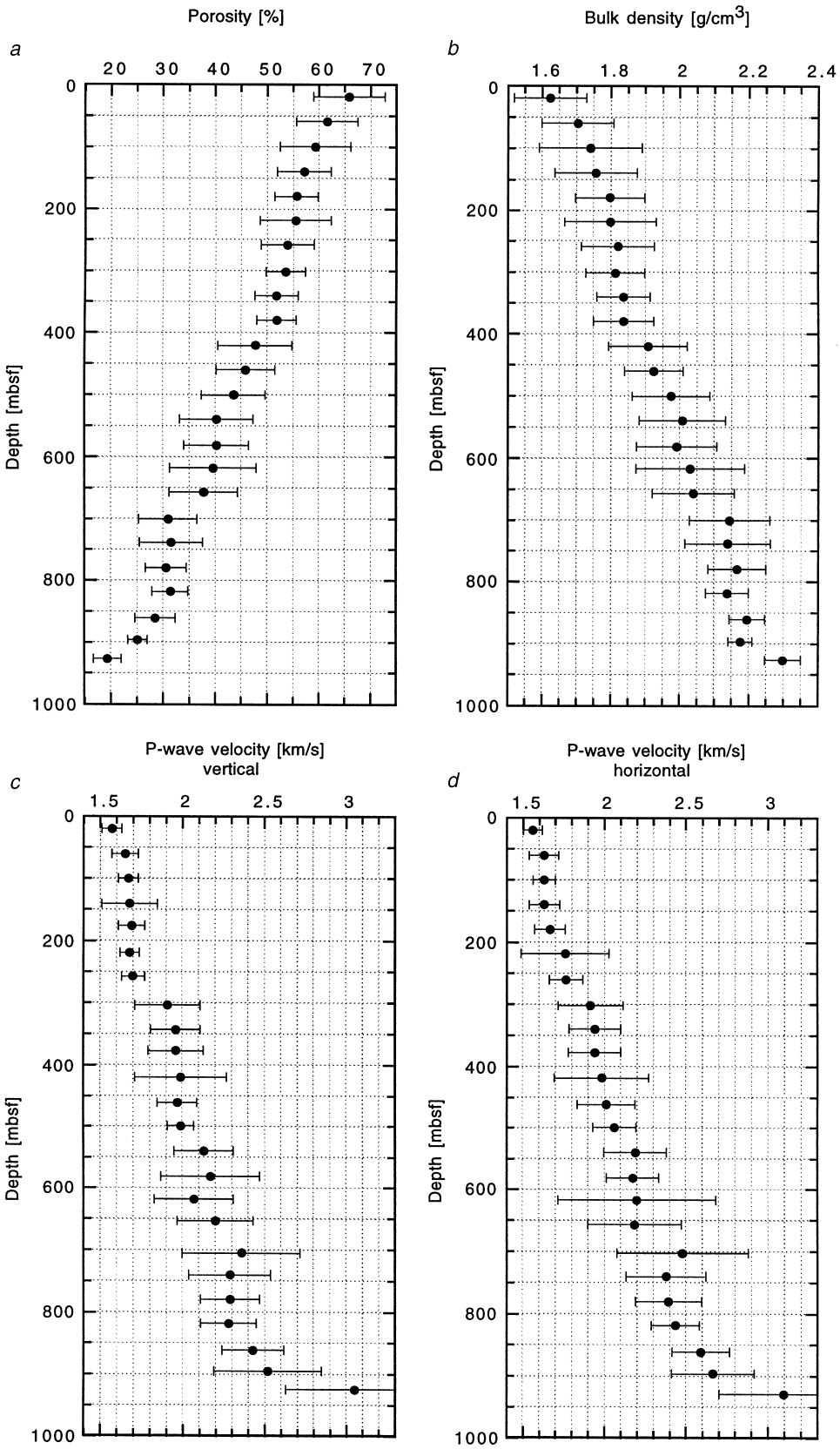

Figure 2—Average values of physical properties with standard deviation for successive 40 m depth intervals. Data are from the drill sites shown in Figure 1.

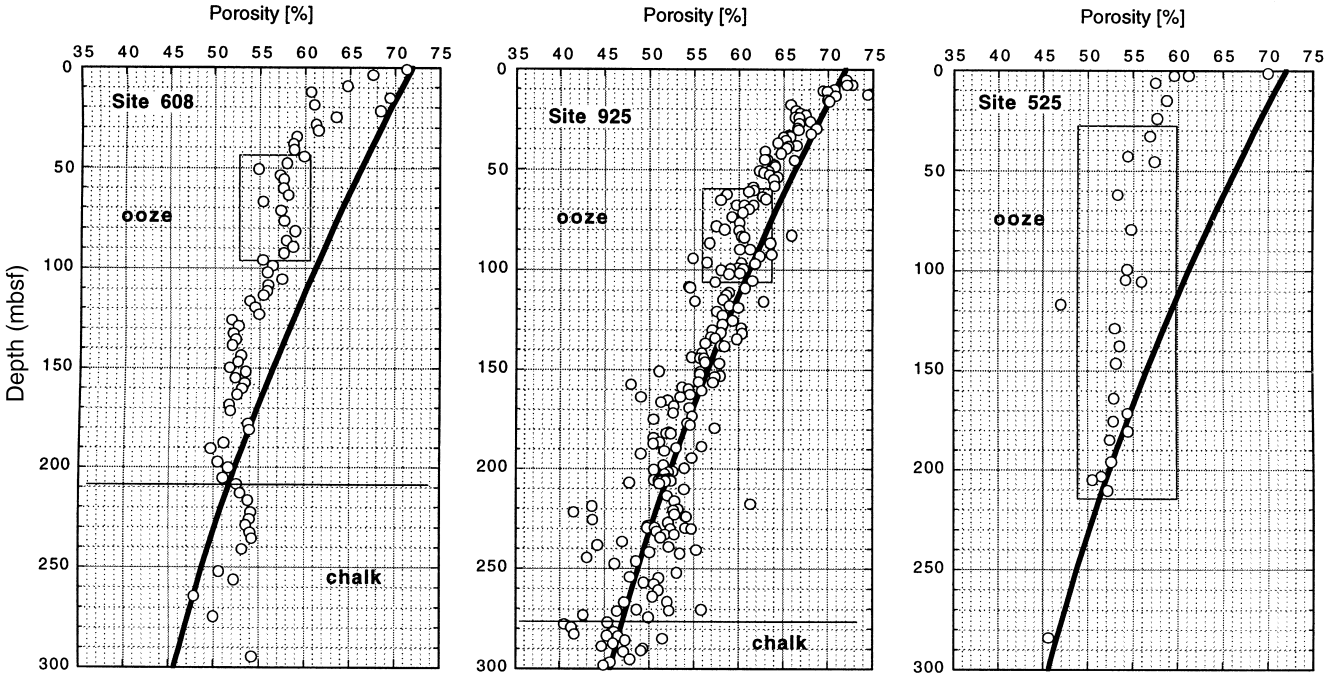

Figure 3—Porosity measurements (circles) from DSDP/ODP Sites 525, 608, and 925 compared to an exponential porosity model (Hamilton, 1976). Hamilton's curve (solid line) fits the data quite well close to the sea floor and at greater depth, but in between there are zones of nearly constant porosity (rectangles) some of which have lower than the predicted porosity. The depth range of these zones and the absolute deviation from the model differ from site to site.

density. The reason acoustic impedance was chosen for this purpose is twofold: (1) acoustic impedance changes show both velocity and density changes and (2) corrected acoustic impedance (dashed line in Figure 6) represents a direct link to seismic stratigraphy. Alternating high and low gradients of acoustic impedance characterize five successive diagenetic stages (Table 3). Using the stratigraphic information given in the DSDP/ODP papers, we were also able to calculate the average duration for each of these diagenetic stages:

Stage I

From the sea floor to 70–100 m subbottom depth, carbonate oozes show high gradients in porosity, bulk density, and sonic velocity (Table 3); consequently, acoustic impedance is increasing rapidly with depth. These changes correlate with pure gravitational compaction of the sediments as reported by numerous workers. Microfossil tests remain largely intact (Figure 5) and the particle size remains constant, whereas the pore volume decreases. The average duration for this compaction process in Atlantic Ocean basins is about 4 m.y.

Stage II

Below 70–100 m burial depth, the effect of gravitational compaction decreases because firm grain contacts are already established. The following depth interval down to 200 m (~4–12 m.y.) is characterized by very low gradients in all recorded physical parameters (Table 3). Diagenesis of carbonate oozes in this interval is characterized by the beginning dissolution of microfossil tests and reprecipitation of calcite. The carbonate particles become smoother because irregular surfaces tend to dissolve. Pore volume remains almost constant because only calcite is involved. A downhole increase in the percentage of broken foraminiferal tests is observed.

Stage III

From 250 down to 700 m burial depth diagenesis is determined by interstitial cementation processes initiated by calcite overgrowth and infillings of remaining tests (Figure 5). In sediments between 12 and 38 m.y. old, chalk becomes the dominant lithology. Chalk diagenesis is accompanied by a strong decrease in porosity and also high gradients in the acoustic parameters (Table 3). During cementation, the particles fuse and grow and the

Table 2. Coefficients Resulting from Polynomial Curve Fits*

	Vertical Velocity		Horizontal Velocity		Bulk Density		Porosity		Impedance	
	Lab	In situ	Lab	In situ	Lab	In situ	Lab	In situ	Lab	In situ
M0	1.510	1.462	1.517	1.461	1.636	1.641	65.351	65.255	2.563	2.532
M1	3.31E-03	3.46E-03	2.26E-03	4.52E-03	–1.46E-03	–1.45E-03	8.04E-02	7.99E-02	–4.98E-03	–6.17E-03
M2	–3.04E-05	3.12E-05	2.56E-05	–2.62E-05	7.04E-05	7.01E-05	–3.93E-03	–3.93E-03	2.96E-04	3.64E-04
M3	5.38E-08	–7.35E-07	–6.73E-07	7.00E-09	–7.13E-07	–7.10E-07	3.94E-05	3.94E-05	–3.61E-06	–4.20E-06
M4	7.87E-10	5.24E-09	4.96E-09	9.91E-10	3.48E-09	3.47E-09	–1.91E-07	–1.91E-07	2.06E-08	2.33E-08
M5	–4.76E-12	–1.83E-11	–1.76E-11	–5.26E-12	–9.56E-12	–9.52E-12	5.24E-10	5.23E-10	–6.40E-11	–7.13E-11
M6	1.16E-14	3.52E-14	3.41E-14	1.23E-14	1.55E-14	1.54E-14	–8.50E-13	–8.48E-13	1.15E-13	1.26E-13
M7	–1.43E-17	–3.81E-17	–3.70E-17	–1.49E-17	–1.47E-17	–1.47E-17	8.10E-16	8.09E-16	–1.18E-16	–1.29E-16
M8	8.91E-21	2.17E-20	2.11E-20	9.20E-21	7.57E-21	7.54E-21	–4.18E-19	–4.17E-19	6.50E-20	7.07E-20
M9	–2.21E-24	–5.04E-24	–4.92E-24	–2.27E-24	–1.62E-24	–1.61E-24	9.00E-23	8.99E-23	–1.47E-23	–1.59E-23
R	0.995	0.997	0.993	0.997	0.995	0.995	0.997	0.997	0.995	0.997

*Of the form $y = M0 + M1 \times z + M2 \times z^2 + \ldots + M9 \times z^9$, z = depth, y = physical property.

pore volume diminishes. The average duration for the cementation process in the Atlantic is approximately 26 m.y.

Stage IV

At 700 m depth, density, porosity, velocity, and acoustic impedance gradients change again to much lower values. At these depth levels, cementation processes leading to chalk and limestone formation are almost completed and further changes occur much slower. Scanning electron micrographs of samples from the depth interval 700–850 m reveal that secondary calcite is already the main constituent of this 38–46-m.y. old sediment (Figure 5).

Stage V

Physical properties change at much higher rates below 850 m depth. At this stage, the sediment consists mainly of secondary calcite crystals (Figure 5) that undergo further gravitational compaction with increasing overburden pressure. In particular, the distinct velocity increase (Table 3) indicates that gravitational compaction of these crystals at depths greater than 900 m (> 46 m.y.) has a strong influence on the elastic parameters of the sediment matrix.

Numerous studies have shown that carbonate diagenesis is a complex interplay of mineralogical and geochemical changes (e.g., Schlanger and Douglas, 1974; Garrison, 1981; Scholle et al., 1991); however, previous physical models of carbonate diagenesis have been quite simple (e.g., Schlanger and Douglas, 1974; Milholland et al., 1980). In most cases these models might be sufficient to estimate, for example, physical property changes when drilling into carbonate deposits; however, the curves presented here, as well as records from single sites in the Atlantic, show that the mineralogical and geochemical complexity of carbonate diagenesis is reflected in changing gradients of physical properties with depth. The empirical depth paths of density, porosity, velocity, and acoustic impedance changes (Figures 4, 6; Tables 2, 3) can be useful predictive models. In an ideal case, it should be possible to predict the diagenetic stage of a drilled carbonate sediment based on physical property measurements; however, we must emphasize that the derived model represents only the average state of carbonate diagenesis in the Atlantic, and data from certain areas can significantly deviate from the model.

Velocity Anisotropy

Velocity anisotropy generally increases with depth during diagenesis (Figure 7). Carlson and

Table 3. Changes of Physical Properties* During Carbonate Diagenesis

	Stage I Compaction of Ooze	Stage II Dissolution of Fossils	Stage III Precipitation of Calcite	Stage IV Further Cementation	Stage V Compaction of Calcite Crystal
Lithology	Ooze	Ooze and chalk	Chalk	Chalk and limestone	Limestone
Depth interval below sea floor (m)	0–100	100–250	250–700	700–850	>850
Time interval (m.y.)	0–4	4–2	12–38	38–46	>46
P-wave velocity vertical					
Average ($m \times s^{-1}$)	1620	1680	2020	2300	2790
Gradient (s^{-1})	1.5	0.4	0.9	0.0	4.4
P-wave velocity horizontal					
Average ($m \times s^{-1}$)	1600	1680	2010	2410	3000
Gradient (s^{-1})	1.0	0.6	1.2	0.7	5.9
Wet bulk density					
Average ($kg \times m^{-3} \times 10^3$)	1.68	1.78	1.93	2.15	2.26
Gradient ($kg \times m^{-4}$)	1.5	0.2	0.7	0.3	3.0
Porosity					
Average (%)	63	56	46	31	24
Gradient ($\% \times m^{-1}$)	–0.08	–0.02	–0.05	–0.02	–0.17
Acoustic impedance					
Average ($kg \times s^{-1} \times m^{-2} \times 10^6$)	2.72	2.99	3.90	4.95	6.31
Gradient ($kg \times s^{-1} \times m^{-3} \times 10^6$)	0.51	0.09	0.34	0.03	1.9

*Average values and depth gradients.

Christensen (1979) suggested that velocity anisotropy in carbonate sediments is caused by alignment of the calcite *c*-axis perpendicular to bedding. Velocity in pure calcite is slowest along the *c*-axis and fastest along the *a*-axis. Several processes may contribute to the alignment of the *c*-axis (Milholland et al., 1980): (1) alignment of discoasters and coccoliths, (2) crushing of foraminifera, and (3) differential crystal overgrowth and cementation (Kamb, 1959). Despite the high variability in our data (high standard deviation), which does not allow for detailed comparison with the above diagenetic stages, Figure 7 shows that the general trend in velocity anisotropy can be subdivided into three zones, which fit with the ooze, chalk, and limestone intervals, respectively. In oozes (0–200 m) anisotropy is slightly negative, but relatively constant, around –2 to 0%, suggesting that gravitational compaction in soft sediments does not have a strong effect on acoustic anisotropy. In the chalk interval (200–700 m), velocity anisotropy exhibits a steady increase to about 8%, indicating increasing alignment of particles parallel to bedding planes. The increase is most likely caused by differential crystal overgrowth because cementation is already the dominant diagenetic process in these depths. Below 700 mbsf, anisotropy remains approximately constant (5–8%), suggesting that maximum alignment of particles is reached in this stage and gravitational compaction of calcite crystals has no further influence on anisotropy. The high scatter in anisotropy can most likely be explained by lithological variability of the noncarbonate fraction in the evaluated sites. Milholland et al. (1980) found that clay enrichment in carbonates can cause an increase in anisotropy possibly because of a catalytic effect on the pressure solution of calcite. Additionally, the anisotropy is a result of preferred orientation of clay particles parallel to the sea floor; however, silica enrichment does not significantly change velocity anisotropy.

The Diagenetic Potential

The degree of lithification of a carbonate sediment at a given depth is determined by the diagenetic potential, a qualitative term introduced by Schlanger and Douglas (1974). At the beginning of the life history of a pelagic carbonate, that is, when calcite is produced by planktonic organisms, the diagenetic potential is very high. During sedimentation to the sea floor and subsequent lithification by compaction and cementation, the diagenetic potential steadily decreases until a zero state is reached in which further diagenetic change is not

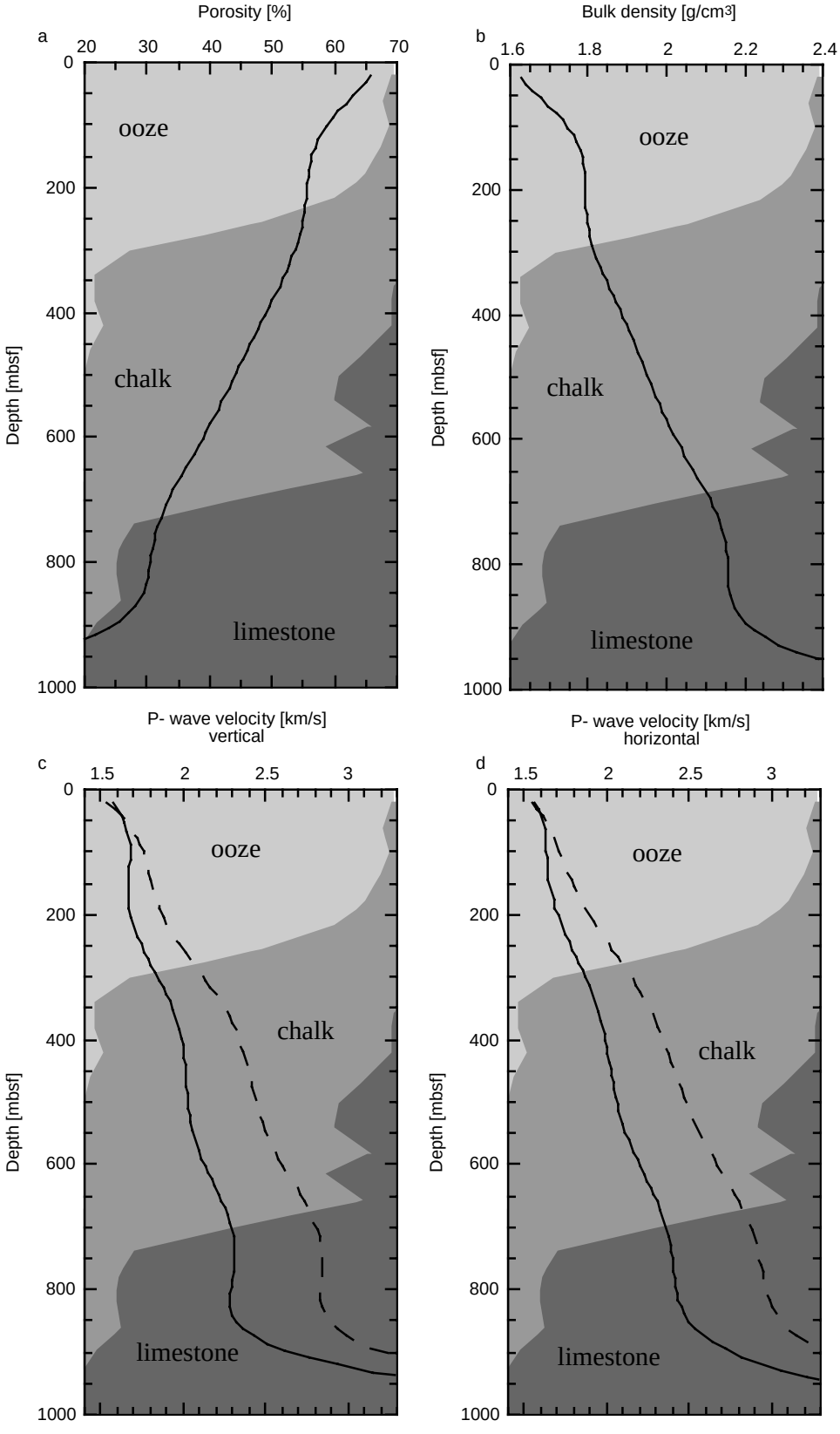

Figure 4—Downhole trends for laboratory (solid lines) and in-situ (dashed lines) physical properties approximated by nine-term polynomial regression (coefficients given in Table 2). For comparison, the relative portions of ooze, chalk, and limestone (from core descriptions) in different depth intervals are plotted in the background of the graph. Increasing lithification is characterized by changing gradients in porosity, density, and velocity with depth.

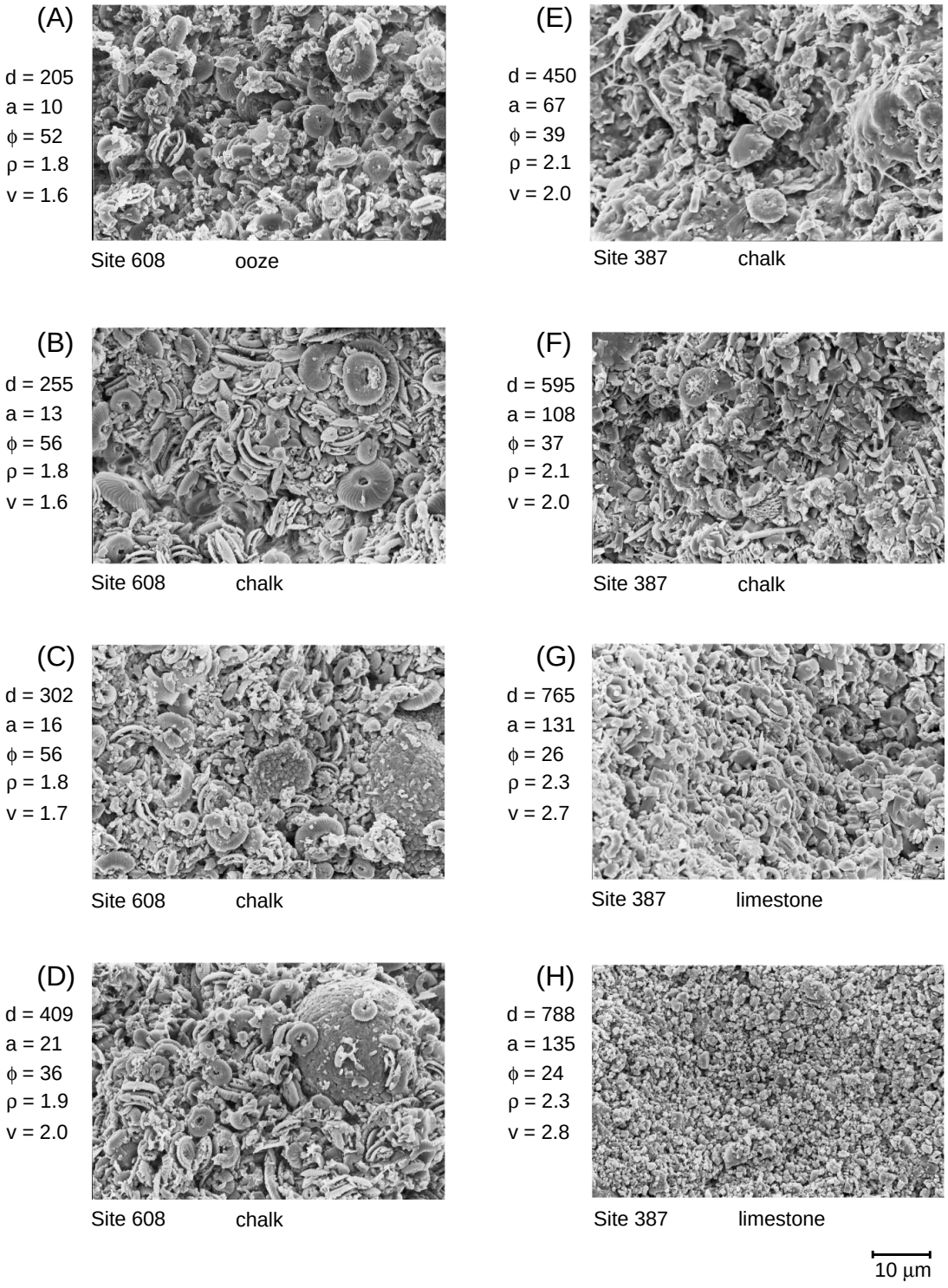

Figure 5—Scanning electron micrographs from carbonate samples of DSDP Sites 608 and 387 document diagenetic changes from ooze to chalk to limestone. Preservation of microfossils in the ooze stage is excellent (A). At deeper burial depths, interstitial cementation processes with calcite overgrowth and infillings of remaining tests lead to increasing lithification of the sediments (B–G) until secondary calcite is the only sediment component. In addition to the micrographs, depth (d), age (a), porosity (ϕ), density (ρ), and horizontal velocity (v) data of the samples are shown.

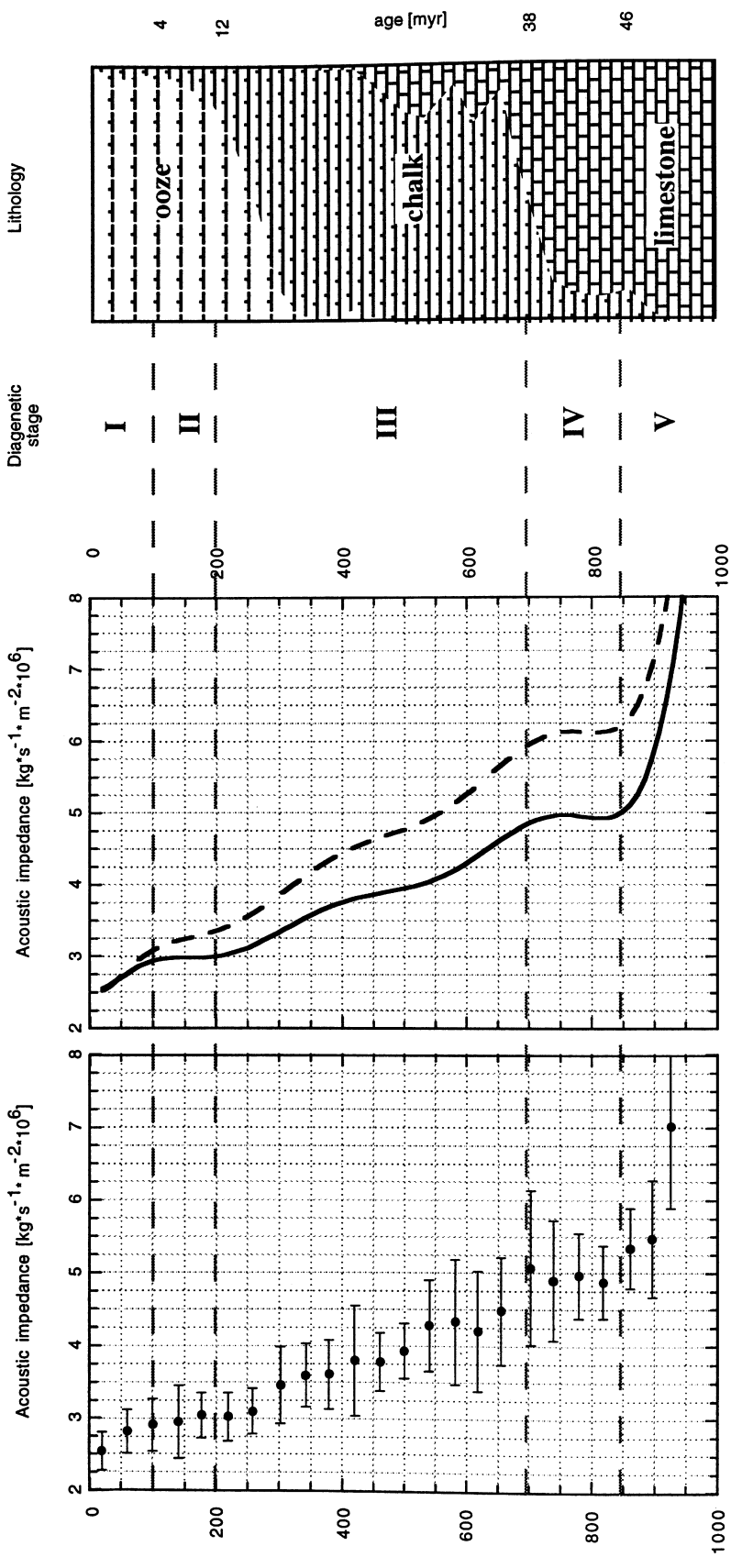

Figure 6—Physical age/depth model of carbonate diagenesis in correlation to lithologic changes. Alternating high and low gradients of impedance characterize five successive diagenetic stages (see also Tables 2, 3). Dots = calculated average laboratory values and standard deviations for successive 40 m depth intervals; solid line = nine-term polynomial regression of laboratory data; dashed line = nine-term polynomial regression of in-situ data.

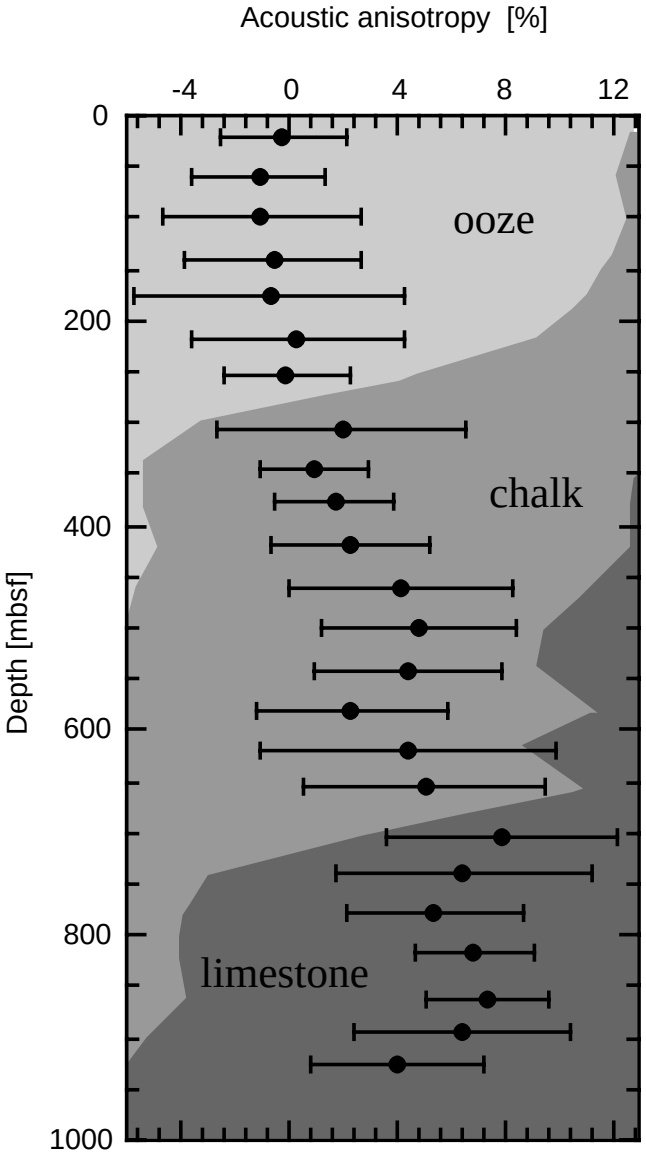

Figure 7—Velocity anisotropy in carbonate sediments calculated from measurements of vertical and horizontal velocity on the same sample and averaged over successive 40 m depth intervals. The general trend in velocity anisotropy can be subdivided into three zones, which fit with the ooze, chalk, and limestone intervals, respectively. The high scatter in anisotropy (high standard deviation) can most likely be explained by lithological variability of the noncarbonate fraction in the evaluated sites.

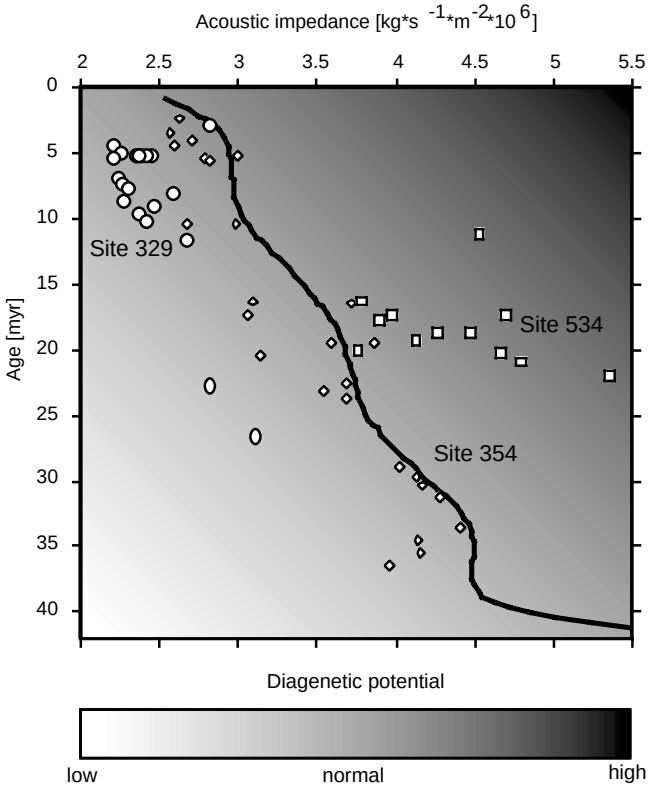

Figure 8—Acoustic impedance as an indicator of diagenetic potential. The impedance vs. age curve derived from our model represents the "normal" diagenetic potential in the Atlantic Ocean. Deviations from this average trend can be interpreted as differences in the initial diagenetic potential of the sediment (indicated by the gray shading). In comparison, DSDP sites with high (534), low (329), and normal (354) diagenetic potential are shown.

possible. Thus, the rate of diagenesis in the sediment column is determined in part by the initial diagenetic potential of the carbonate particles; hence, differences in lithification observed in carbonate sediments of the same age can be explained by differences in the sea floor diagenetic potential. The diagenetic potential is controlled by a variety of factors, such as water depth, sedimentation rate, surface productivity, foraminifer to coccolith ratio, etc. The extensive data set evaluated here allows quantification of the differences in lithification and thus presents a more quantitative estimate of the diagenetic potential. This is illustrated in Figure 8, where acoustic impedance is used as a measure of lithification with age. The impedance vs. age curve (solid line) is based on the entire data set. It was constructed analog to the impedance vs. depth curve in Figure 6 (polynomial fit) and represents the change of "normal" diagenetic potential in the Atlantic Ocean. Deviations from this average trend can be interpreted as differences in the initial diagenetic potential of the sediment, as indicated by the gray shading in Figure 8. For example, siliceous carbonate oozes and chalks of sections from DSDP Site 329 (western Maurice Ewing bank) display a relatively low acoustic impedance compared to the acoustic impedance predicted from the model for

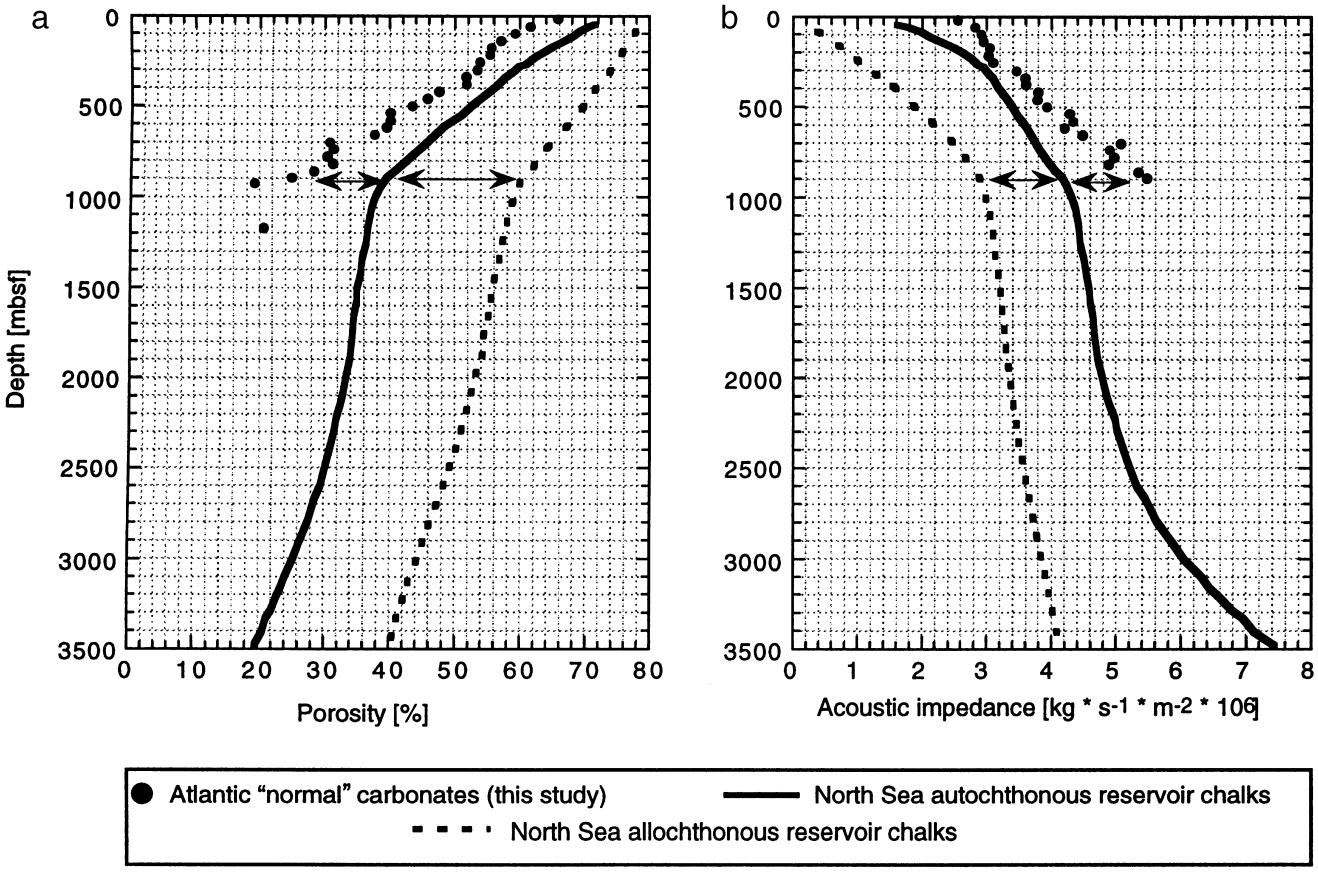

Figure 9—(a) Porosity (modified after Brasher and Vagle, 1996) and (b) acoustic impedance of Atlantic "normal" carbonates and chalk reservoirs (allochthonous and autochthonous) vs. burial depth. Below 1000 m, gradients of porosity and impedance change to significantly lower values due to overpressuring and the influence of hydrocarbon migration. The diagenetic potential of these sediments remains low.

Table 4. Comparison of Reservoir and Nonreservoir Chalk Types

	Atlantic "Normal" Carbonates (This Study)	North Sea Autochthonous Reservoir Chalks	North Sea Allochthonous Reservoir Chalks
Depth (km)	0.9	3	3
Porosity (%)	22	26	44
Density ($kg \times m^{-3} \times 10^3$)	2.27	2.21	1.95
Velocity (m/s)	3120	2790	2030
Acoustic impedance ($kg \times s^{-1} \times m^{-2} \times 10^6$)	7.08	6.17	3.96
Diagenetic stage	V	IV–V	III
Diagenetic potential	Normal	Low	Very low

Miocene carbonates. This difference is caused largely by the low initial diagenetic potential at this Site 329, which is controlled by the relatively shallow burial of the chalks due to slow sedimentation and erosion; however, chalk of the same age from Site 534 (Blake-Bahama Basin) exhibit high acoustic impedance. These chalks were deposited as clasts by repeated debris flows. Thus, the high initial diagenetic

potential at this site is mainly caused by chalk type. An example of sediments with "normal" diagenetic potential are nannofossil oozes and chalks from Site 354 (Ceara rise).

Reservoir Quality and Diagenetic Potential

The degree of compaction and cementation plays an integral part in defining the ultimate quality of a reservoir rock because porosity retention or occlusion depends on the degree to which these processes occur. The derived physical models of the diagenetic potential can indirectly help determine reservoir qualities of chalks. To demonstrate this, we compare our model to published data from the greater Ekofisk area. This prominent marine carbonate reservoir consists of Cretaceous and Tertiary chalks (e.g., D'Heur, 1986; Kennedy, 1987) and is located within the southern Norwegian sector of the North Sea.

In the North Sea Central Graben, chalks were deposited as hemipelagic oozes composed of coccolithophorids, along with planktonic and benthonic foraminifera. Intercalated into these autochthonous chalks are sediment packages that were rapidly deposited by slumps, slides, debris flows, and turbidites (Watts et al., 1980). These allochthonous bodies comprise both clean and argillaceous chalks and tend to have better reservoir properties than the autochthonous units (e.g., Taylor and Lapré, 1987). Brasher and Vagle (1996) generated general curves for porosity reduction in pure autochthonous and pure allochthonous reservoir chalks with increasing burial depth based on empirical field data (Figure 9a). Case studies from North Sea oil fields reveal that the porosity reduction of specific fields, such as Edda, Tor, and Eldfisk, usually falls between these two "extreme" curves. We have used Brasher and Vagle's (1996) porosity data together with sonic and formation density logs from a variety of studies (Norwegian Petroleum Directorate, 1981; D'Heur, 1986; Sørensen et al., 1986; Kennedy, 1987) to calculate curves for the acoustic impedance of allochthonous and autochthonous chalk reservoirs (Figure 9b). Both North Sea chalk types display higher initial porosity (lower impedance, lower initial diagenetic potential), but roughly parallel the diagenetic pathway predicted by our model (Atlantic "normal" carbonates) in the upper 1000 m below the sea floor. Below 1000 m, North Sea chalks clearly did not progress along the "normal" trend given by the model (Figure 9). Gradients of porosity and impedance change to significantly lower values due to overpressuring and the influence of hydrocarbon migration. In other words, the diagenetic potential of these sediments remains low. Overpressuring results from rapid basin subsidence and lowers the effective stresses at grain contacts, thus reducing mechanical and chemical compaction. At the level of hydrocarbon migration, the cementation halts because dissolution and precipitation of $CaCO_3$ were inhibited; therefore, porosity and impedance were largely preserved and the diagenetic potential is minimal because diagenesis is extremely slow.

The low diagenetic potential of chalk reservoirs is further illustrated by Table 4, which compares different chalk types of Paleocene–Cretaceous age. Normal Atlantic carbonates of this age today are in diagenetic stage V (compaction of calcite crystals) and occur at average depth of about 900 m. North Sea reservoir chalks of the same age are buried much deeper and therefore a higher diagenetic potential (low porosity, high impedance) is expected, but the effects of overpressuring and hydrocarbon migration on the diagenetic potential exceed that of burial depth, so that physical properties of autochthonous and allochthonous reservoir chalks are equivalent to earlier diagenetic stages IV (cementation) and III (precipitation of calcite), respectively.

CONCLUSIONS

Physical property measurements on ooze, chalk, and limestone samples from DSDP/ODP sites in Atlantic Ocean basins have been integrated to derive a new physical model that accounts for mineralogical changes observed during carbonate diagenesis.

The general downhole trend of increasing acoustic parameters (velocity, density, acoustic impedance) and decreasing porosity exhibits successive intervals that are characterized by alternating high and low depth gradients. These intervals have been correlated to published studies concerning textural changes, fossil preservation, and sediment age. Five stages of carbonate diagenesis can be identified and described by physical property changes: (1) compaction of ooze (0–100 m, 0–4 m.y., high gradients), (2) breakage and dissolution of fossil tests (100–250 m, 4–12 m.y., low gradients), (3) formation of chalk through precipitation of calcite (250–700 m, 12–38 m.y., high gradients), (4) further cementation (700–850 m, 38–46 m.y., low gradients), and (5) compaction of calcite crystals (>850 m, >46 m.y., high gradients).

Our proposed model describes physical property changes with nine-term polynomial equations and can predict values of density, porosity, velocity (vertical and horizontal), and acoustic impedance down to a burial depth of 1000 m. The primary model, based on measurements at laboratory conditions,

also has been adjusted to in-situ conditions, allowing comparison of the model with physical properties derived from laboratory, downhole, and seismic methods.

Changes in velocity anisotropy, calculated from measurements of vertical and horizontal velocity on the same sample, suggest that differential crystal overgrowth during cementation in chalks has a much greater affect on acoustic anisotropy than compaction processes in oozes and limestones.

A more quantitative expression of the diagenetic potential, a qualitative term introduced by Schlanger and Douglas (1974), has been derived from the model by using an impedance vs. age curve to estimate the degree of lithification. The derived models can indirectly be used to estimate reservoir quality of carbonate reservoirs. We demonstrated that North Sea chalk reservoirs are characterized by a very low diagenetic potential.

REFERENCES CITED

Audet, D. M., 1995, Modelling of porosity evolution and mechanical compaction of calcareous sediments: Sedimentology, v. 42, p. 355–373.

Bassinot, F. C., J. C. Marsters, L. A. Mayer, and R. H. Wilkens, 1993, Variations of porosity in calcareous sediments from the Ontong Java Plateau, *in* W. H. Berger, L. W. Kroenke, and L. A. Mayer, eds., Proceedings of the Ocean Drilling Program, scientific results, 130: College Station, Texas, Ocean Drilling Program, p. 653–661.

Berger, W. H., 1974, Deep-sea sedimentation, *in* C. A. Burk and C. L. Drake, eds., The geology of continental margins: New York, Springer-Verlag, p. 213–241.

Borre, M., I. Lind, and J. Mortensen, 1996, Specific surface as a measure of burial diagenesis of chalk: Terra Nostra, Schriften der Alfred-Wegener-Stiftung, v. 96, no. 4, p. 24–25.

Boyce, R. E., 1973, Appendix I; physical properties—methods, *in* N. T. Edgar, J. B. Saunders et al., eds., Initial Reports of the Deep-Sea Drilling Project: Washington, U.S. Government Printing Office, v. 15, p. 1115–1128.

Boyce, R. E., 1976a, Sound velocity-density parameters of sediment and rock from DSDP drill sites 315–318 on the Line Island chain, Manihiki Plateau and Tuamotu Ridge in the Pacific Ocean, *in* S. O. Schlanger, et al., eds., Initial Reports of the Deep-Sea Drilling Project: Washington, D.C., U.S. Government Printing Office, v. 33, p. 695–728.

Boyce, R. E., 1976b, Definitions and laboratory techniques of compressional sound velocity parameters and wet-water content, wet bulk density, and porosity parameters by gravimetric and gamma ray attenuation techniques, *in* S. O. Schlanger, et al., eds., Initial Reports of the Deep-Sea Drilling Project: Washington, D.C., U.S. Government Printing Office, v. 33, p. 931–958.

Brasher, J. E., and K. R. Vagle, 1996, Influence of lithofacies and diagenesis on Norwegian North Sea chalk reservoirs: AAPG Bulletin, v. 80, p. 746–769.

Carlson, R. L., and N. I. Christensen, 1977, Velocity anisotropy and physical properties of deep-sea sediments from the western South Atlantic, *in* P. R. Supko, et al., eds., Initial Reports of the Deep-Sea Drilling Project: Washington, D.C., U.S. Government Printing Office, v. 39, p. 555–559.

Carlson, R. L., and N. I. Christensen, 1979, Velocity anisotropy in semi-indurated calcareous deep-sea sediments: Journal of Geophysical Research, v. 84, p. 205–211.

D'Heur, M., 1984, Porosity and hydrocarbon distribution in the North Sea chalk reservoirs: Marine and Petroleum Geology, v. 1, p. 211–238.

D'Heur, M., 1986, The Norwegian chalk fields, *in* A. M Spencer, E. Holter, S. O. Johnson, A. Mørk, E. Nysaether, P. Songstad, and A. Spinnagr, eds., Habitat of hydrocarbons on the Norwegian continental shelf: London, Graham and Trotman, p. 77–89.

Fischer, A. G., S. Honjo, and R. W. Garrison, 1967, Electron micrographs of limestones and their nannofossils: Princeton, Princeton University Press, 137 p.

Garrison, R. E., 1981, Diagenesis of oceanic carbonate sediments: a review of the DSDP-perspective, *in* J. E. Warme, R. G. Douglas, and E. L. Winterer, eds., The Deep-Sea Drilling Project: a decade of progress: SEPM Special Publication 32, p. 181–207.

Hamilton, E. L., 1965, Sound speed and related physical properties of sediments from experimental MOHOLE (Guadalupe Site): Geophysics, v. 30, p. 257–261.

Hamilton, E. L., 1976, Variations of density and porosity with depth in deep-sea sediments: Journal of Sedimentary Petrology, v. 46, p. 280–300.

Hempel, P., L. A. Mayer, E. Taylor, G. Bohrmann, and A. Pittenger, 1989, The influence of biogenic silica on seismic lithostratigraphy at ODP Sites 642 and 643, eastern Norwegian Sea, *in* O. Eldholm, et al., eds., Proceedings of the Ocean Drilling Program, Scientific Results, 104; College Station, Texas, Ocean Drilling Program, p. 941–951.

Kamb, W. B., 1959, Theory of preferred crystal orientation developed by crystallization under stress: Journal of Geology, v. 67, p. 153–170.

Kennedy, W. J., 1987, Sedimentology of Late Cretaceous–Palaeocene chalk reservoirs, North Sea Central Graben, *in* J. Brooks and K. Glennie, eds., Petroleum Geology of north west Europe, London, Graham and Trotman, v. 1, p. 469–481.

Kim, D.-C., M. H. Manghnani, and S. O. Schlanger, 1985, The role of diagenesis in the development of physical properties of deep sea carbonate sediments: Marine Geology, v. 69, p. 69–91.

Mackenzie, K. V., 1981, Nine-term equation for sound speed in the oceans: Journal of the Acoustical Society of America, v. 70, no. 3, p. 807–812.

Marsters, J. C., and M. H. Manghnani, 1993, Consolidation test results and porosity rebound of Ontong Java Plateau sediments., *in* W. H. Berger, L. W. Kroenke, and L. A. Mayer, eds., Proceedings of the Ocean Drilling Program, Scientific Results, 130: College Station, Texas, Ocean Drilling Program, p. 687–694.

Matter, A., R. G. Douglas, and K. Perch-Nielsen, 1975, Fossil preservation, geochemistry and diagenesis of pelagic carbonates from Shatsky rise, northwest Pacific, *in* R. L. Larson, et al., eds., Initial Reports of the Deep-Sea Drilling Project: Washington, D.C., U.S. Government Printing Office, v. 32, p. 891–922.

Mayer, L. A., R. C. Courtney, and K. Moran, 1987, Novel acoustics applications/seafloor engineering, *in* P. Meyboom and E. Lawder, eds., The ocean; an international workplace: Proceedings, New York, Institute of Electrical and Electronics Engineers, p. 1–5.

Mazullo, S. J., and P. M. Harris, 1992, Mesogenetic dissolution: its role in porosity development in carbonate reservoirs: AAPG Bulletin, v. 76, p. 607–620.

Milholland, P., M. H. Manghnani, S. O. Schlanger, and G. H. Sutton, 1980, Geoacoustic modelling of deep sea carbonate sediments: Journal of the Acoustical Society of America, v. 68, p. 1351–1360.

Norwegian Petroleum Directorate, 1981, The Eldfisk Area: Norwegian Petroleum Directorate paper v. 30, 35 p.

Schlanger, S. O., and R. G. Douglas, 1974, The pelagic ooze-chalk-limestone transition and its implications for marine stratigraphy, *in* K. J. Hsü and H. C. Jenkyns, eds., Pelagic sediments on land and under the sea: International Association of Sedimentologists Special Publication no. 1, p. 117–148.

Scholle, P. A., 1977, Chalk diagenesis and its relation to petroleum exploration: oil from chalks, a modern miracle: AAPG Bulletin, v. 61, p. 982–1009.

Scholle, P. A., L. Stemmerik, and D. S. Ulmer, 1991, Diagenetic history and hydrocarbon potential of Upper Permian carbonate

buildups, Wegener Halvø area, Jameson Land basin, East Greenland: AAPG Bulletin, v. 75, p. 701–725.
Shipley, T. H., 1983, Physical properties, synthetic seismograms, and seismic reflection correlation at DSDP Site 534, Blake-Bahama basin, *in* J. P. Kennett, et al., eds., Initial Reports of the Deep-Sea Drilling Project: Washington, D.C., U.S. Government Printing Office, v. 76, p. 653–665.
Sørensen, S., M. Jones, R. F. P. Hardman, W. K. Leutz, and P. H. Schwarz, 1986, Reservoir characteristics of high- and low-productivity chalks from the central North Sea, *in* A. M. Spencer, E. Holter, S. O. Johnson, A. Mørk, E. Nysaether, P. Songstad, and A. Spinnagr, eds., Habitat of hydrocarbons on the Norwegian continental shelf: London, Graham and Trotman, p. 91–110.
Taylor, S. R., and J. F. Lapré, 1987, North Sea chalk diagenesis: its effect on reservoir location and properties, *in* J. Brooks and K. Glennie, eds., Petroleum Geology of northwest Europe, London, Graham and Trotman, v. 1, p. 483–496.
Urmos, J., 1994, Diagenetic and physical properties of pelagic carbonate sediments: ODP Leg 130, Ontong Java Plateau: Ph.D. thesis, University of Hawaii, Honolulu, 213 p.
Urmos, J., and R. H. Wilkens, 1993, In situ velocities in pelagic carbonates: new insights from Ocean Drilling Program Leg 130, Ontong Java Plateau: Journal of Geophysical Research, v. 98, p. 7903–7920.
Urmos, J., R. H. Wilkens, F. Bassinot, M. Lyle, J. Marsters, L. Mayer, and D. Mosher, 1993, Laboratory and well-log velocity and density measurements from the Ontong Java Plateau: new in-situ corrections to laboratory data from pelagic carbonates, *in* W. H. Berger, L. W. Kroenke, and L. A. Mayer, eds., Proceedings of the Ocean Drilling Program, Scientific Results, 130: College Station, Texas, Ocean Drilling Program, p. 607–621.
van der Lingen, G. J., and G. H. Packham, 1975, Relationships between diagenesis and physical properties of biogenic sediments of the Ontong-Java Plateau (Sites 288 and 289, Deep-Sea Drilling Project), *in* J. E. Andrews, et al., eds., Initial Reports of the Deep-Sea Drilling Project: Washington, D.C., U.S. Government Printing Office, v. 30, p. 443–481.
Watts, N. L., J. F. Lapré, F. S. van Schijndel-Goester, and A. Ford, 1980, Upper Cretaceous and lower Tertiary chalks of the Albuskjell area, North Sea: deposition in a slope and base-of-slope environment: Geology, v. 8, p. 217–221.
Wise, S. W., 1973, Calcareous nannofossils from cores recovered during Leg 18, Deep-Sea Drilling Project: biostratigraphy and observations of diagenesis, *in* L. D. Kulm, et al., eds., Initial Reports of the Deep-Sea Drilling Project: Washington, D.C., U.S. Government Printing Office, v. 18, p. 569–615.
Wyllie, M. R. J., A. R. Gregory, and L. W. Gardner, 1956, Elastic wave velocities in heterogeneous and porous media: Geophysics, v. 21, p. 41–70.

ABOUT THE AUTHORS

Jens Grützner

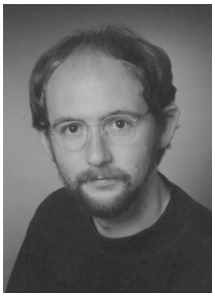

Jens Grützner has a degree in geophysics from the University of Hamburg, Germany, and a Ph.D from the University of Kiel, Germany. Since 1990, he has been with GEOMAR Research Center for Marine Geosciences in Kiel, where he has been working on a variety of research projects related to the sediments of Atlantic Ocean basins using physical property measurements and reflection seismics. He participated in Legs 154 and 172 of the Ocean Drilling Program. His current interests are in sediment diagenesis, paleoceanography, and nondestructive core logging methods.

Jürgen Mienert

Jürgen Mienert received a Ph.D. from the University of Kiel. He was at research institutions in the United States at the Lamont-Doherty Earth Observatory (1981–1982) and at Woods Hole Oceanographic Institution (1985–1998), and in Germany at the GEOMAR Research Center at Kiel University (1988–1998). He is now a full professor in applied geophysics and arctic marine geology at the Department of Geology at the University of Tromsø. He has carried out research on continental margins and the deep sea using high-resolution reflection seismics, high-resolution ocean bottom seismometers, high-resolution side-scan sonar, coring, and deep-sea drilling. His present research focuses on the development of glaciated and nonglaciated margins regarding stability zones of both hydrates and sediments inferred from geophysical and geological records.